Formation and physicochemical properties of crystalline and amorphous salts with different stoichiometries formed between ciprofloxacin and succinic acid

Krzysztof J. Paluch[a], Thomas Mc Cabe[b], Helge Muller-Buntz[c], Owen I. Corrigan[a], Anne Marie Healy[a], Lidia Tajber[a*]

a) School of Pharmacy and Pharmaceutical Sciences,
b) School of Chemistry, Trinity College Dublin, College Green, Dublin 2, Ireland,
c) School of Chemistry and Chemical Biology, University College Dublin, Belfield, Dublin 4.

*To whom correspondence should be sent. Ph.: +35318962787, e-mail: lidia.tajber@tcd.ie

Abstract

Multi-ionisable compounds, such as dicarboxylic acids, offer the possibility of forming salts of drugs with multiple stoichiometries. Attempts to crystallise ciprofloxacin, a poorly water soluble, amphoteric molecule with succinic acid (S) resulted in isolation of ciprofloxacin hemisuccinate (1:1) trihydrate (CHS-I) and ciprofloxacin succinate (2:1) tetrahydrate (CS-I). Anhydrous ciprofloxacin hemisuccinate (CHS-II) and anhydrous ciprofloxacin succinate (CS-II) were also obtained. It was also possible to obtain stoichiometrically equivalent amorphous salt forms, CHS-III and CS-III, by spray drying and milling, respectively, of the drug and acid. Anhydrous CHS and CS had melting points at ~215 and ~228 °C, while the glass transition temperatures of CHS-III and CS-III were ~101 and ~79 °C, respectively. Dynamic solubility studies revealed the metastable nature of CS-I in aqueous media, resulting in a transformation of CS-I to a mix of CHS-I and ciprofloxacin 1:3.7 hydrate, consistent with the phase diagram. CS-III was observed to dissolve non-congruently leading to high and sustainable drug solution concentrations in water at 25 and 37 ºC, with the ciprofloxacin concentration of 58.8±1.18 mg/ml after 1 hour of the experiment at 37 ºC. This work shows that crystalline salts with multiple stoichiometries and amorphous salts have diverse pharmaceutically-relevant properties, including molecular, solid state and solubility characteristics.

Key words: ciprofloxacin, succinic acid, solubility, ternary phase diagram, single crystal X-ray, dynamic vapour sorption, morphology.

1. Introduction

Ciprofloxacin (C), 1-cyclopropyl-6-fluoro-4-oxo-7-(piperazin-1-yl)-quinoline-3-carboxylic acid (Fig. 1), is a widely used second generation fluoroquinolone antibacterial compound for the treatment of bacterial infections of the lower respiratory tract and skin tissue.

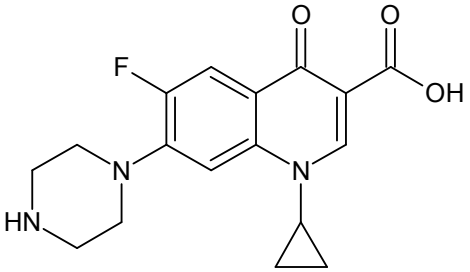

Figure 1. Chemical structure of ciprofloxacin.

C is a class IV of the Biopharmaceutics Classification System drug[1], predominantly absorbed in the proximal part of the gastrointestinal tract (GIT).[2] The aqueous solubility of C is pH-dependent, due to the presence of the carboxylic and NH groups of piperazine, with the zwiterionic and unionised forms being dominant at neutral pH.[3] Since solubility is one of the properties which directly impacts on bioavailability of an active pharmaceutical ingredient (API), salt formation using suitable counterions is an approach often employed to improve the aqueous solubility of drugs. Indeed, C is commercially available as a hydrochloride 1.4-hydrated salt, the structure of which has been described by Turel and Golobic.[4] However, hydrochloride salts often suffer from a decreased solubility in the stomach due to a common ion effect.[5] Taking the above into consideration, alternative forms of C, which do not contain the chloride counterion and

exhibit high solubility at the pH of the absorption site (the upper part of the GIT) might therefore be useful.

Preparation of C salts with organic acids such as citric, tartaric and malonic acid has previously been presented.[6] Recently, we reported on the ability of another amphoteric molecule, salbutamol, to form a salt with succinic acid or a cocrystal of salbutamol adipate salt with adipic acid.[7] All of the above examples of counterions include organic acids with more than one carboxylic group, potentially presenting the possibility of the formation of salts with multiple stoichiometries. While, in theory, it is possible to predict whether multiple stoichiometries are likely to form, based on the chemical structure of the drug and counterion, it is not yet possible to predict if salts with different stoichiometries will crystallise.[8] Mono- and bis-hydrochloride salts of GSK159797 have been reported.[9] Tamoxifen has been isolated as a 1:1 (molar ratio) anhydrous citrate salt as well as a sesquihydrate with the 2:1 molar ratio of the drug to the counterion.[10] Multiple stoichiometries of succinic salts of a pleuromutilin derivative have also been characterised.[11] The ciprofloxacin salts obtained by Reddy et al. were of 1:1 drug:acid stoichiometry only.[6] Succinic acid, due to its pK_a values close to each other (4.21 and 5.64)[12] and thus greater likelihood of di-anion formation, may be a better counterion to study the potential of ciprofloxacin (pK_a values of 6.09 and 8.74)[13] to form salts with multiple stoichiometries.

Guerrieri et al. stated that amorphous salts might provide an opportunity to enhance dissolution behaviour in biological fluids due to a higher solubility of the ionised drug in comparison to the nonionised form and the higher apparent solubility of the amorphous form.[14] Although amorphous forms of salts are known, the published studies

have primarily concentrated on investigations of the solid state properties, including the work of Guerrieri et al. on procaine salts.[14] Examples include the work of Tong et al. on correlating the glass transition temperature (Tg) of amorphous alkali metal salts of indomethacin with the size/charge ratio of the counterion.[15] In another study the Tgs, crystallisation tendency and moisture sorption behaviour of amorphous salts of nicardipine or propranolol were systematically investigated however no apparent trends between these parameters and the counterions used were evident.[16] Sonje et al., in addition to an extensive account on the Tgs, fragility and devitrification tendency of amorphous salts of atorvastatin manufactured by spray drying, concluded that greater dissolution rates, in comparison to the crystalline counterparts, were obtained using amorphous salts of magnesium and calcium, but not sodium.[17] Hasa et al. obtained a rapidly and highly absorbed amorphous salt, vinpocetine citrate, by neat co-grinding a mix of the drug and the acid in the presence of amorphous polymer, crospovidone.[18]

Consequently, the aim of this work was to explore the possibility of crystalline ciprofloxacin salt formation with succinic acid with an emphasis on screening whether this drug molecule can form salts with multiple stoichiometries. Also, considering that only very limited information on pharmaceutically-relevant properties of amorphous salts can be found, to manufacture the amorphous counterparts of any ciprofloxacin succinate form(s) and compare the physicochemical properties of the various forms.

2. Materials and methods

2.1. Materials

Ciprofloxacin (anhydrous, Fluka, China) later referred to as C, succinic acid (S) (Aldrich, USA), water (Millipore Elix 3 UK), ethanol (Corcoran Chemicals, Ireland), potassium bromide, sodium chloride, sodium hydroxide and triethylamine (Sigma-Aldrich, Germany), 85% phosphoric acid, 37% hydrochloric acid, sodium dihydrogen phosphate dihydrate and Karl-Fischer universal reagent (Riedel de Haen, Germany), HPLC acetonitrile and HPLC methanol (Fischer Scientific, UK).

2.2. Methods

2.2.1. Production of salts

2.2.1.1. Preparation of crystalline bulk materials

Ciprofloxacin hemisuccinate (1:1) trihydrate (CHS-I) was crystallised by cooling a 80 ml aqueous solution of 3 mmol anhydrous ciprofloxacin (C) and 3 mmol succinic acid (S) from 70 °C to 4 °C at a rate of 1 °C/min.

Ciprofloxacin succinate (2:1) tetrahydrate (CS-I) was crystallised by cooling a 50% v/v ethanolic solution (50% ethanol/50% water v/v) containing C and S in the 1:1 molar ratio from 70 °C to 4 °C (1 °C/min). In order to avoid conversion of C to C-I (ciprofloxacin hydrate), 1.5 mmol S was first dissolved in 20 ml pure water and then heated to 70 °C. 1.5 mmol C was dissolved in the warm solution of S and the required amount of warm ethanol (at 70 °C) was added to form the 50% v/v ethanolic solution.

Anhydrous ciprofloxacin hemisuccinate (CHS-II) was crystallised by evaporation of a 1:1 (molar ratio) aqueous solution of C and S under reduced pressure (-80 mbar) at 70 °C using a rotary evaporator (Büchi Rotavapor R-210, Flawil, Switzerland).

Anhydrous ciprofloxacin succinate (CS-II) was obtained by tray drying of CS-I in an oven (Memert, Germany) for 6 hours at 70 ˚C, until the mass loss recorded by thermogravimetric analysis (TGA) was lower than 1% w/w in the temperature range of 25-150 ˚C at a heating rate of 10 ˚C/min.

2.2.1.2. Preparation of single crystals

In order to grow the crystals of CHS-I and CS-I of sufficient size and quality for the single crystal X-ray diffraction analysis, the liquid diffusion method was used.[19] An aqueous solution of S and C (1:1 molar ratio), saturated at room temperature, was covered in a glass vial with a layer of pure ethanol. The ethanol layer was applied very gently to form two layers of liquids. Equal volumes of the liquids were used. Crystals of both phases grew at the boundary layer of the ethanol and aqueous solution.

2.2.1.3 Spray drying

The feed solutions were prepared by dissolving C and S in the 1:1 molar ratio in water and spray dried using a Büchi B-290 Mini Spray dryer (Flawil, Switzerland). The drying gas (compressed, dehumidified air for open mode and nitrogen for closed mode) pressure was 6 bar at 4 cm gas flow (rotameter setting), equivalent to 473 norm litres per hour (NL/h) of gas flow in normal conditions (p=1013.25 mbar and T=273.15 K).[20] A standard atomization nozzle with a 1.5 mm cap and 0.7 mm tip was employed for processing. The nozzle pressure drop was measured to be 0.41 bar. The pump speed was set to 30% (9-10 ml/min) and the aspirator was operated at 100%. The Inert Loop Büchi B-295 was used to spray dry in the closed mode configuration and its temperature was set to 20 °C. The solution feed concentration used was 1%, 1.5% or 2% (w/v) and the inlet

temperature 80, 120, 140, 160, 170 or 180 °C resulting in an outlet temperature ranging from 38 to 98 °C depending on the combination of process parameters used.

2.2.1.4 Milling

Amorphous CS-III was prepared by dry milling a physical mix of C and S (2:1 molar ratio) at room temperature using a planetary ball mill PM 100 (Retsch, Haan, Germany) at 600 rpm speed. The powder to ball weight ratio was 1:48 as 2 g of powder was loaded to the stainless steel milling container which had a volume of 50 ml and three stainless steel balls (20 mm in diameter, 32 g each) were used for all milling experiments.

2.2.2. Single crystal X-ray diffraction (SCXRD)

Crystal data were collected using an Agilent Technologies (former Oxford Diffraction) SuperNova A diffractometer fitted with an Atlas detector. CHS-I was measured with Cu-Kα (1.54184 Å), CS-I with Mo- Kα (0.71073 Å). A complete (CS-I) or fivefold redundant (CHS-I) dataset was collected, assuming that the Friedel pairs are not equivalent. An analytical absorption correction based on the shape of the crystal was performed.[21] The structures were solved by direct methods using SHELXS-97[22] and refined by full matrix least-squares on F2 for all data using SHELXL-97.[22] Hydrogen atoms were added at calculated positions and refined using a riding model. Their isotropic temperature factors were fixed to 1.2 times (1.5 times for methyl groups) the equivalent isotropic displacement parameters of the carbon atom the H-atom is attached to. Anisotropic thermal displacement parameters were used for all non-hydrogen atoms. To evaluate the data, Mercury 2.2 software was used.[23]

2.2.3. Powder X-ray diffraction (PXRD)

Powder XRD analysis was conducted using a Rigaku MiniflexII Desktop X-ray diffractometer (Tokyo, Japan) with Haskris cooling unit (Grove Village, IL, USA). The tube output voltage used was 30 kV and tube output current was 15 mA. A Cu-tube with Ni-filter suppressing Kβ radiation was used. Measurements were taken from 5 to 40 on the 2 theta scale at a step size of 0.05˚ per second in each case.[24] Scans were performed at room temperature. All PXRD measurements were performed in duplicate.

2.2.3.1. Calculation of crystallite shapes

To calculate the theoretical crystallite shapes of the materials, PXRD patterns were analysed using Peak Search software (Rigaku, Japan). Baseline noise was corrected and relative intensities of Bragg peaks were calculated. Collected data was analysed using VESTA software (ver. 3.1.1)[25] as described by Izumi and Momma.[26]

2.2.4. Differential scanning calorimetry (DSC)

DSC experiments were performed using a Mettler Toledo DSC 821e (Schwerzenbach, Switzerland) with a refrigerated cooling system LabPlant RP-100 (Filey, UK). Nitrogen was used as the purge gas. Aluminium sample holders (40 μL) were sealed with a lid and pierced to provide three vent holes. Sample volume was sufficient to provide proper contact between the powder and the bottom of the pan, and sample weight was ≥5 mg. DSC measurements were carried out at a heating/cooling rate of 10 ˚C/min.[27] The unit was calibrated with indium and zinc standards. All DSC measurements were performed in triplicate. All DSC results presented are those obtained at 10 ˚C/min unless stated otherwise.

2.2.4.1. Temperature modulated differential scanning calorimetry (MT-DSC StepScan™)

A PerkinElmer Diamond DSC unit (Waltham, MA, USA) with HyperDSC was implemented to detect glass transition temperatures of amorphous systems.[28] The unit was refrigerated using an ULSP B.V. 130 cooling system (Ede, Netherlands) and operated under a nitrogen flow of 40 ml/min. The gas flow was controlled using a PerkinElmer Thermal Analysis Gas Station (TAGS). Samples were heated at 5˚C/min in 2 ˚C steps. Between each of the dynamic steps a 1 minute isothermal step was applied. The area algorithm was applied to calculate the specific heat of glass transition from the enthalpy flow. A baseline run was performed for each sample to minimise sample holder mass error. Samples were tested in 18 µL aluminium holders sealed with pierced lid to provide three vent holes. Sample volume was sufficient to provide proper contact between powder and a pan bottom, never less than 5 mg. The unit was calibrated with indium and zinc standards. Presented results are the average of triplicate analyses.

2.2.4.2 High speed DSC (HSDSC)

HSDSC measurements were carried out using a PerkinElmer Diamond DSC unit with HyperDSC described as above. Heating rates of 10, 50, 100, 200, 300, 400 and 500 °C/min were used with nitrogen (10 ºC/min, 40 ml/min) or helium (other heating rates, 60 ml/min) as the purge gas. The samples were prepared as explained in Section 2.2.4.1. Presented results are the average of triplicate analyses.

2.2.5. Thermogravimetric analysis (TGA)

TGA was performed using a Mettler TG 50 (Schwerzenbach, Switzerland) module linked to a Mettler MT5 balance. Samples were placed into open aluminium pans (5-12 mg). A heating rate of 10 ˚C/min was implemented in all measurements.[27] Analysis was carried out in the furnace under nitrogen purge and monitored by Mettler Toledo

STARe software (version 6.10) with a Windows NT operating system. All TGA measurements were performed in triplicate.

2.2.6. Karl Fischer (KF) titrimetry

0.5 g of sample was dissolved in pre-titrated 50 ml of methanol. Metrohm 841 Titrando (Herisau, Switzerland) was used for titration and the unit was calibrated with 20 µl of water.[29] Presented results are the average of triplicate analyses.

2.2.7. Solid state Fourier transform infrared spectroscopy (FTIR)

Infrared spectra were recorded on a Nicolet Magna IR 560 E.S.P. spectrometer (Madison, WI, USA) equipped with a MCT/A detector, working under Omnic software version 4.1. A spectral range of 650-4000 cm^{-1}, resolution 2 cm^{-1} and accumulation of 64 scans were used in order to obtain good quality spectra. A KBr disk method was used with a 0.5-1% sample loading. KBr disks were prepared by direct compression under 8 bar pressure for 1 minute.[30] All FTIR measurements were performed in duplicate. The sample preparation did not affect the spectra, as confirmed with an attenuated total reflectance (ATR) spectrometer (data not shown).

2.2.9. Gas chromatography – mass spectrometry (GC-MS)

A known weight of each sample was placed in a headspace vial to which 1 ml of deionised water was added. The vials were sealed. The vials were then heated and agitated at 80 ˚C for 10 minutes in a headspace auto-sampler where the volatile organics in the samples were driven into the headspace of the vial (the air above the sample). 1 ml of the headspace gas was then extracted by syringe from the vial and injected onto the GC-MS Varian Saturn 220 (CA, USA). Ethanol eluted at 8.1 minutes. The column used

for the analysis was a WCOT fused Silica 60 m x 0.32 mm ID coating CP-SELECT 624 CB, df=1.8 μm. GC-MS measurements were performed in triplicate.

2.2.10. Dynamic vapour sorption (DVS)

Vapour sorption experiments were performed on a DVS Advantage-1 automated gravimetric vapour sorption analyser (Surface Measurement Systems Ltd., London, UK). The DVS-1 measures the uptake and loss of water vapour gravimetrically with a mass resolution of ± 0.1 μg. The temperature was maintained constant at 25.0 ± 0.1 °C. A mass of around 10 mg of powder was loaded into a sample net basket and placed in the system. The samples were equilibrated at 0% of relative humidity (RH) until dry, reference mass was recorded. The samples were exposed to the following % of RH profile: 0 to 90% in 10% steps and the same for desorption. At each stage, the sample mass was equilibrated ($dm/dt \leq 0.002$ mg/min for at least 10 min) before the change of relative humidity. An isotherm was calculated from the complete sorption and desorption profile. All DVS measurements were performed in duplicate.

To determine the critical relative humidity of crystallisation of amorphous salts, the sample was exposed to the following relative humidity rates: 2.5, 5, 10 and 15% RH/h. The critical relative humidity was established as previously described.[31,32] Briefly, an isotherm was calculated from the complete sorption profile. The amount of sorbed water was expressed as a percentage of the dry mass. Crystallisation of the material was indicated by the points of inflection. %RH of crystallisation were then plotted versus ΔRH%/h and linearly extrapolated to 0 ΔRH%/h.

2.2.11. Solubility and ternary phase diagram studies

2.2.11.1 Equilibrium solubility studies

The solubilities of C, S and salts were determined by adding the solid in approximately a 3-fold excess of the amount expected to achieve saturated solubility into an Eppendorf tube and adding 2 ml of solvent.[7] The Eppendorf vials were then hermetically sealed, placed horizontally in a water bath at 25 ºC and shaken at 100 cpm. After 24 h the suspensions were filtered through a 0.45 μm PVDF membrane filter[7] and the content of constituents in the supernatant was determined by HPLC (Section 2.2.13). The solubility samples were prepared and tested at least in triplicate.

2.2.11.2 Dynamic solubility studies

Dynamic solubility studies were performed in 20 ml glass vials placed in jacketed beakers to control temperature (either 25 or 37 ºC). 5 ml of water was added to each of the vials and the solid under investigation was added in approximately a 3-fold excess of the expected saturated solubility. Aliquots of the suspension were withdrawn at predetermined intervals, filtered through a 0.45 μm PVDF membrane filter[7] and the content of the drug and the acid in the solution phase was determined by HPLC (Section 2.2.13). The pH of the aqueous saturated solutions was measured using a Thermo Orion 420+ pH-meter (Thermo Scientific, Hampshire, UK). The experiments were repeated at least in triplicate. The remaining solid material at the end of the solubility studies (equilibrium and dynamic) was separated from the liquid by filtration and analysed using PXRD.

2.2.12.1. Construction of a ternary phase diagram

A series of mixes of C, S and deionised water containing a varied proportion of the components were prepared in 20 ml capped glass vials. The vials were then placed horizontally in a water bath at 25 ºC and shaken at 100 cpm. After 24 h the suspensions

were filtered through a 0.45 μm PVDF membrane filter and the content of the drug and the acid in the solution phase was determined by HPLC (Section 2.2.13). Each experiment was repeated at least in duplicate. The remaining solid phase (if present) was analysed by PXRD. The equilibrium solubility of C and S was determined as described in Section 2.2.11.1.

2.2.13. High performance liquid chromatography (HPLC)

The content of ciprofloxacin was determined using the HPLC method described in the British Pharmacopeia.[33] The content of succinic acid was determined using the conditions previously described.[7] Briefly, a Shimadzu 10Avp HPLC system (Tokyo, Japan) was employed and the separation was done at room temperature. For ciprofloxacin the analytical column used was a C18(2) Luna column (250 mm length, internal diameter 4.6 mm, and particle size 5 μm). The mobile phase was composed of a 2.45 g/l solution of phosphoric acid, previously adjusted to pH 3.0 with triethylamine mixed with acetonitrile (87:13 v/v). A flow rate of 1.5 ml/min with the UV detection at 278 nm was used. For succinic acid the analytical column used was a LiChrosorb RP-10 column (250 mm length, internal diameter 4 mm, and particle size 10 μm). UV detection was carried out at a wavelength of 210 nm and the injection volume was 10 μl. Separation of succinic acid was carried out using a gradient method with a flow rate of 1 mL/min. The mobile phase consisted of two eluents: (A) phosphoric acid solution (pH 2.1) and (B) methanol and a pH=2.1 phosphoric acid solution [20:80 (v/v)]. The following gradient was used: a linear gradient from 0% to 50% B over 7 min, and then a linear gradient from 50% to 100% B over 1 min; this composition was maintained for 7 min. Then, again a linear gradient from 100% to 0% B over 10 min was applied, and the final mobile phase

composition was continued further for 5 min. Each sample was measured in duplicate and each solution was injected in duplicate.

2.2.14. Scanning Electron Microscopy (SEM)

SEM analysis was performed using a Zeiss SUPRA Variable Pressure Field Emission scanning electron microscope (Jena, Germany). The resolution was 3 nm at 30 kV, accelerating voltage was 5 kV and the detector used was the secondary electron detector. Samples were glued onto aluminium stubs and sputter-coated with gold under vacuum prior to analysis.

2.2.15. Data analysis

The crystallographic data was analysed in detail using Ortep-3[34], Platon[35] and CrystalExplorer (ver.3.0)[36] software. The statistical significance of the differences between samples was determined using one-way analysis of variance (ANOVA) followed by the posthoc Tukey's test using Minitab software. Differences were considered significant at $p < 0.05$.

3. Results and discussion

3.1 Production of crystalline and amorphous salts

A solid phase, later referred to as CHS-I (ciprofloxacin hemisuccinate (1:1) trihydrate), was found to crystallise from a solution of C and S dissolved in the 1:1 molar ratio in water. Since succinic acid is a diprotic acid, attempts to obtain a 2:1 ciprofloxacin succinate form were made from a solution of C and S dissolved in the 2:1 molar ratio in water by evaporative (slow) and cooling (as described in Section 2.2.1.1) crystallisation processes. These attempts were unsuccessful and yielded mixtures of CHS-I and another solid, later identified as a hydrated form of ciprofloxacin and referred to as C-I. Also

reaction crystallisation[37] experiments (at room temperature), whereby varying amounts of C powders were added to a saturated solution of S in water and water/ethanol mixtures, were fruitless. However, when cooling crystallisation from ethanolic solutions was devised, it was observed that 50% v/v ethanolic solution containing C and S in the 1:1 molar ratio resulted in the isolation of a solid, later referred to as CS-I (ciprofloxacin succinate (2:1) tetrahydrate). A 0.5 molar excess of S was necessary to prevent C-I crystallisation prior to the formation of CS-I. Higher concentrations of ethanol were also effective, but resulted in unnecessary dilutions of the crystallisation medium. It is therefore interesting that the 1:1 and 2:1 crystalline salts crystallised from the same drug:acid stoichiometry in solution, with only the solvent system being different.

Anhydrous CHS and CS forms, later referred to as CHS-II and CS-II, were obtained by drying CHS-I and CS-I and, in addition, CHS-II was found to form upon crystallisation under reduced pressure from a solution of C and S dissolved in the 1:1 molar ratio in water.

Spray drying was investigated as a method to generate amorphous forms of ciprofloxacin succinate however, due to the very low solubility of the drug in common process solvents, this method was employed to process aqueous solutions containing C and S in the 1:1 molar ratio only. Samples spray dried from higher feed concentrations (2% w/v) were PXRD amorphous, while those dried from lower feed concentrations (1 and 1.5% w/v) and the sample processed in the closed mode configuration were partially crystalline (Fig. 2). The variation in the inlet temperature employed (120-180 °C) did not have a noticeable effect on amorphisation of the CS phase, impacting only the content of residual water in the spray dried material, which varied from 3.0-0.8% w/w. HPLC

showed no chemical degradation of ciprofloxacin on processing. The amorphous sample spray dried from a 2% w/v solution of C and S present in the 1:1 molar ratio at an inlet temperature of 140 °C (Fig. 2e) was used for further analysis and is referred to as CHS-III.

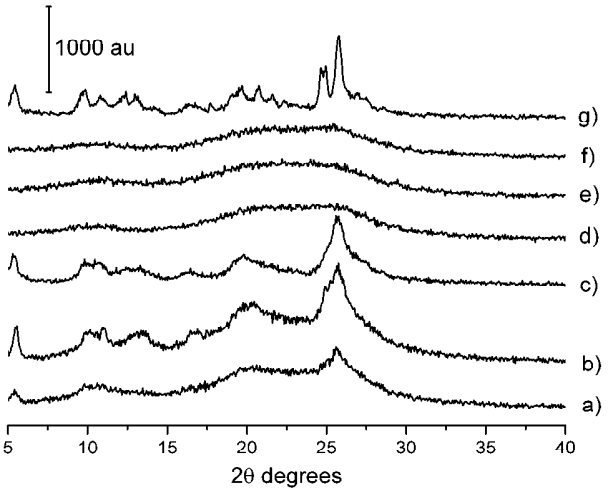

Figure 2. PXRD patterns of ciprofloxacin (C) and succinic acid (1:1 molar ratio) spray dried at the following conditions (solid concentration, inlet temperature): a) 1.5% w/v, 160 °C, b) 1.5% w/v, 170 °C, c) 1% w/v, 180 °C, d) 2% w/v, 120 °C, e) 2% w/v, 140 °C (CHS-III), f) 2% w/v, 160 °C and g) 2% w/v, 80 °C (closed mode configuration).

Amorphous ciprofloxacin succinate 2:1, later referred to as CS-III, was produced by planetary ball milling due to drug solubility limitations. PXRD and DSC were applied to determine the milling time sufficient to produce the amorphous phase, which was 6 h (Fig. 3). HPLC confirmed that the drug remained intact in all milled samples, thus ciprofloxacin did not decompose on processing. Mechanochemistry by neat and solvent-drop grinding, as one of the screening tools for obtaining crystalline salts, has been advocated by Trask et al.[38] Various combinations of a counterion and either trimetoprim or pyrimethamine were co-ground using a Retsch mixer mill MM200 and the efficiency of the process in terms of the successful production of a crystalline salt was reported to be

approximately 40% for neat grinding, increasing to 100% for solvent-drop grinding.[38] The mechanical energy and shearing forces generated in the mill allow solid-state reactions to be conducted.[18] Hasa et al. described the process of mechanochemical salt formation of amorphous vinpocetine citrate and vincamine citrate based on dry co-grinding physical mixtures of the base and the acid containing either crospovidone[18] or sodium carboxymethyl cellulose.[39]

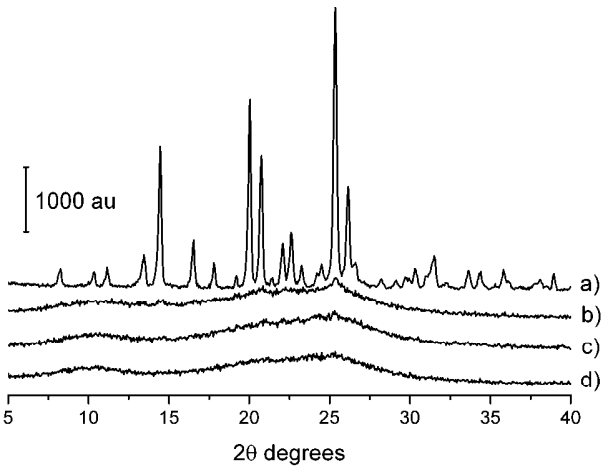

Figure 3. PXRD patterns of ciprofloxacin (C) and succinic acid (2:1 molar ratio): a) unprocessed, starting mixture (0 h), b) milled for 2 h, c) milled for 4 h and d) milled for 6 h (CS-III).

A summary of the various solid-state forms of ciprofloxacin discussed in this manuscript is presented in Table 1.

Table 1. The solid state forms of ciprofloxacin considered in this manuscript.

Symbol	Name	Space group a b c	Cell volume α β γ	Theoretical water content [%]
*C	Ciprofloxacin anhydrous[40]	P-1 7.9606(2) 8.5798(2) 10.7739(3)	732.431 87.868(3) 85.153(2) 88.212(1)	0
*C-I	Ciprofloxacin 1:3.7 (3:11) hydrate[41]	P-1 13.8921(4) 15.0770(5) 16.2208(5)	2751.22 111.4970(10) 105.9840(10) 106.1990(10)	16.6
CHS-I	Ciprofloxacin hemisuccinate (1:1), trihydrate	P-1 7.3528(2) 9.5471(2) 16.5419(4)	1138.05 79.038(2) 87.943(2) 86.992(2)	10.7
CHS-II	Ciprofloxacin hemisuccinate (1:1), anhydrous	N/A		0
CHS-III	Ciprofloxacin succinate (1:1), anhydrous, amorphous	N/A		0
CS-I	Ciprofloxacin succinate (2:1), tetrahydrate	P-1 9.5788(3) 13.6952(5) 17.0039(5)	1978.72 68.041(3) 83.225(3) 73.039(3)	8.5
CS-II	Ciprofloxacin succinate (2:1), anhydrous	N/A		0
CS-III	Ciprofloxacin succinate (2:1), anhydrous, amorphous	N/A		0

* denotes ciprofloxacin forms characterised previously

3.2. Structural analysis of CHS-I and CS-I

The unit cell, determined by SCXRD, of ciprofloxacin hemisuccinate (1:1) trihydrate (CHS-I) (Table 1, Table SI.1, Fig. SI.1) is packed with two molecules of the drug and two molecules of the acid with six molecules of water placed interstitially. The aromatic cores of the drug molecules are π-stacked along the crystallographic a-axis at 3.59 Å distance. The plane of the cyclopropyl ring (C16-C18) of ciprofloxacin is located

at an angle of 118.2(1)° to the plane of the quinoline ring (the C1-C5-N1 fragment) and the torsion angle for C1-N1-C16-C18 is 43.6(2)°.

Only one carboxylic group per every molecule of S is deprotonated, which is confirmed by the fact that between the O4 or O5 oxygen atoms and the C19 carbon are almost the same distances, at 1.269(2) Å and 1.249(2) Å, respectively (Fig. 4a). We previously reported full deprotonation of succinic acid in salbutamol succinate, with C-O bond distances of 1.274(1) and 1.253(2) Å.[7] In the second carboxylic group of S, which is protonated, the interatomic distance for O6-C22 is 1.211(2) Å and C22-O7 is 1.324(2) Å. The length of the protonated single C-O bond and C=O bond in the carboxylic group of adipic acid in the cocrystal of salbutamol hemiadipate salt with adipic acid was 1.322(2) and 1.213(2) Å, respectively.[7]

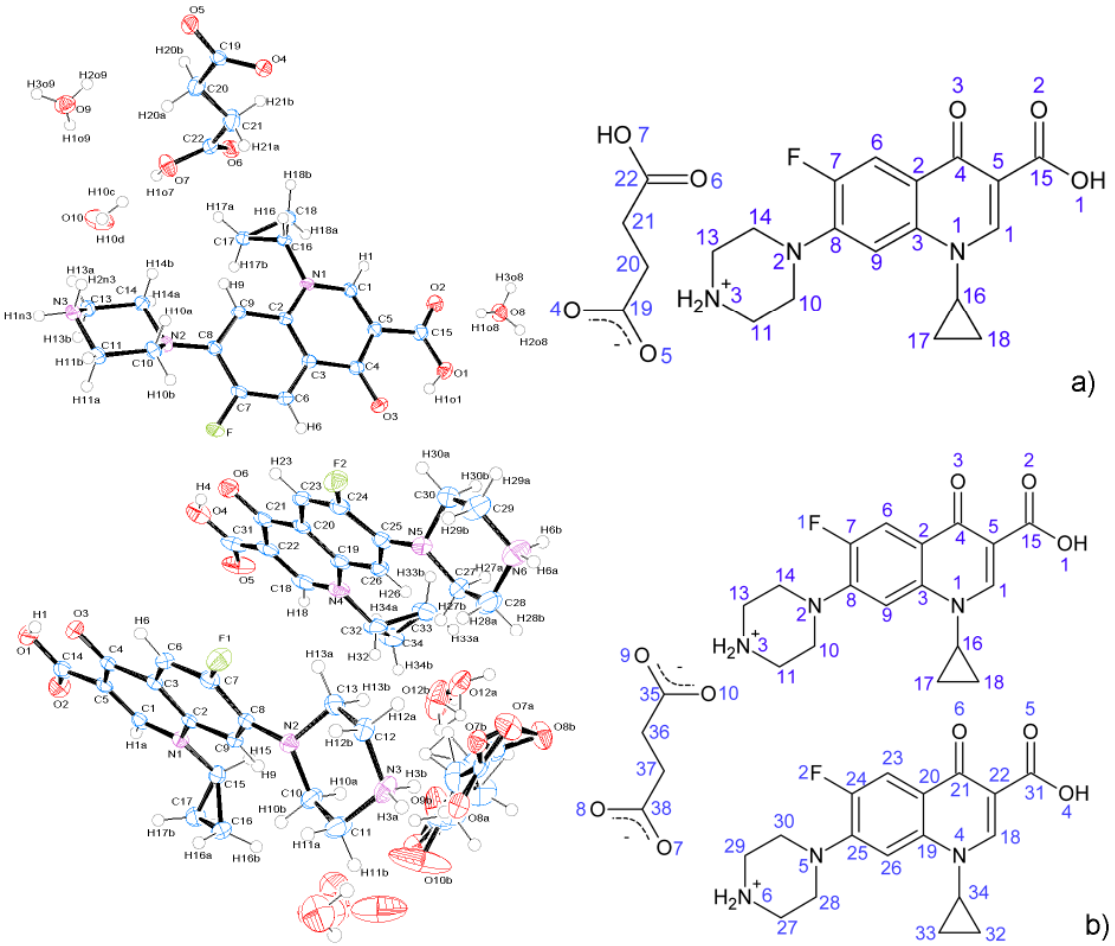

Figure 4. Ortep view with 50% probability ellipsoids (left) and numbered chemical structures (right) of: a) CHS-I and b) CS-I. Water molecules are not included in the numbered chemical structures for clarity.

The deprotonated carboxylic group of S forms hydrogen bond with the protonated amine group (N3…O5: 2.710(2) Å) as well as with the carboxylic acid (O7…O4: 2.513(1) Å). Remarkably the protonated oxygen of the acid (O7) acts not only as a H-bond donor, but also as an acceptor from a water molecule (O10…O7: 2.954(2) Å). The water molecules, the protonated amine and the carboxylic acid form a complex three-dimension hydrogen bond network. There is also an intramolecular H-bond formed between O3 of the ketone group and H1o1 of the neighbouring carboxylic group attached

to the quinoline ring (1.746(1) Å). Details of other H-bonds in CHS-I are presented in Table SI.2.

In general, the H-bond network in CHS-I explored by Hirshfeld surface analysis[42] is mainly formed through H-O and H-H interactions which cover 34.0% and 41.1%, respectively, of the whole Hirshfeld surface, presented as d_{norm} reciprocal interactions[43] (Fig. 5).

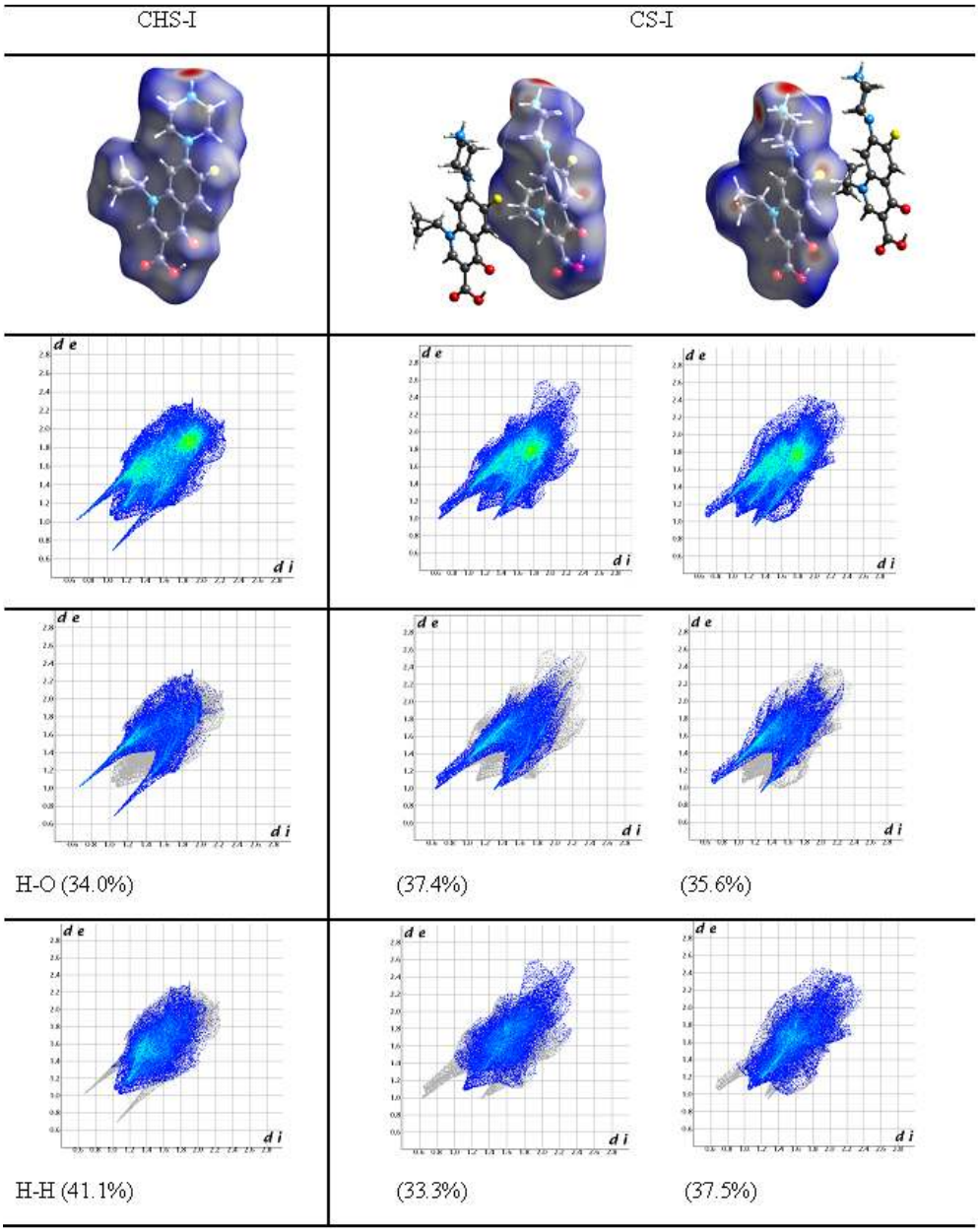

Figure 5. Hirshfeld surface analysis of ciprofloxacin molecules in CHS-I (left column) and CS-I (right column, the data for the two crystallographically independent drug molecules is presented separately). Top row presents the Hirshfeld surface of ciprofloxacin molecule, second row shows the total fingerprint plot of the drug molecule, while the third and bottom rows present the % of reciprocal O-H and H-H contacts, respectively, in the fingerprint plot of the drug molecule.

The unit cell of ciprofloxacin succinate (2:1) tetrahydrate (CS-I) (Table 1, Table SI.1) is packed with four molecules of the drug, two disordered molecules of the acid and twelve molecules of water (Fig. SI.3). CS-I has a layered structure, whereby the drug layers alternate along the b-direction with the layers containing the acid and water molecules. π-stacking extends along the crystallographic b-axis at a distance of 3.83 Å. The two molecules of drug in CS-I are crystallographically independent (Fig. 4b) and later referred to as CPR(1) and CPR(2) based on the label number of the fluorine (F) atom, thus Hirshfeld surface analysis was performed for both drug molecules separately. The contribution of the H-H contacts in the CPR(1) molecule in comparison to ciprofloxacin in CS-I decreased to 33.3% and for the CPR(2) molecule to 37.5% (Fig. 5). In contrast, the coverage of the H-O contacts increased to 37.4% and 35.6% for the CPR(1) and CPR(2), respectively. The differences are directly related to the rearrangement of the hydrogen bonds network and short range contacts as well as the differences in the geometry of ciprofloxacin molecules in comparison to CS-I.

The crystal structure of CS-I presents two cases of disorder. The first is related to the molecule of water with O12A and O12B, the second was found in the molecule of succinic acid. The disorder in S (Fig. SI.5) comprises two crystallographically independent acid molecules (C35-C38) A and B. The torsion angle C35-C36-C37-C38 in the molecule A is -173(1)°, while in the molecule B the torsion angle has an opposite sign (+173(1)°). This angle is different by 6° when compared to that of the acid molecule in CHS-I.

The extensive disorder in the succinate anion makes it difficult to determine whether both carboxylic acid groups in both orientations are fully deprotonated. Large

thermal ellipsoids indicate that the positions of the oxygen atoms, especially O9 and O10 in both orientations, are rather ill-defined, i.e. the carbon-oxygen bond lengths are somewhat uncertain. However, in both ciprofloxacin molecules the protons attached to the piperazine nitrogens (N3 and N6) were clearly visible in the electron density map. This is an indication that N3 and N6 are both fully protonated, so the carboxylate groups must all be fully deprotonated.

In CS-I the protonated amine of CPR-1 forms hydrogen bonds to the succinate only (via H3A: N3…O7A: 2.765(5) Å, N3…O7B: 2.705(4) Å; via H3B: N3…O7B: 2.883(5) Å, N3…O8A: 2.600(3) Å). Similar intramolecular hydrogen bonds as in CHS-I are present (O1…O3: 2.558(2) Å, O4…O6: 2.540(2) Å). The one of CPR-2 forms hydrogen bonds to the succinate via H6A (N6…O9B: 2.598(5) Å; N6…O10A:2.846(4) Å) and to a water via H6B (N6…O11: 2.763(3) Å). These bonds are stabilised by a complex network of hydrogen bonds involving also water molecules as presented in Table SI 3.

Pharmaceutical examples of succinate salts comprising the singly ionised succinate moiety include: doxylamine succinate[44], sumatriptan succinate[45], strychnine succinate[46], desvenlafaxine succinate[47], imiquimod succinate[48], in contrast metoprolol succinate[49] has the counterion double ionised, i.e. both of the carboxylic acid groups are deprotonated. Therefore it appears that monodissociated succinic acid prevails in pharmaceutical succinate salts and CS-I is a rare example of a salt comprising a fully dissociated succinic acid residue.

3.3 Physicochemical properties of crystalline salts

The experimental PXRD pattern of CHS-I (Fig. 6d) was superimposable with that calculated from the single crystal analysis (Fig. 6c) and both were different to the diffractograms of parent compounds, C and S (Fig. 6a and b). The powder pattern of ciprofloxacin starting material used in this study superimposed with the theoretical powder pattern of anhydrous ciprofloxacin reported by Fabbiani et al.[40] Also, the diffractogram of CHS-I was different to that of ciprofloxacin hydrate (Fig. SI.6) observed to form in some crystallisation experiments (as described in Section 3.1). This form was named C-I and was identified as the 1:3.7 hydrate of the drug.[41] The PXRD pattern of CS-I (Fig. 6h) was also different to that of C and S.

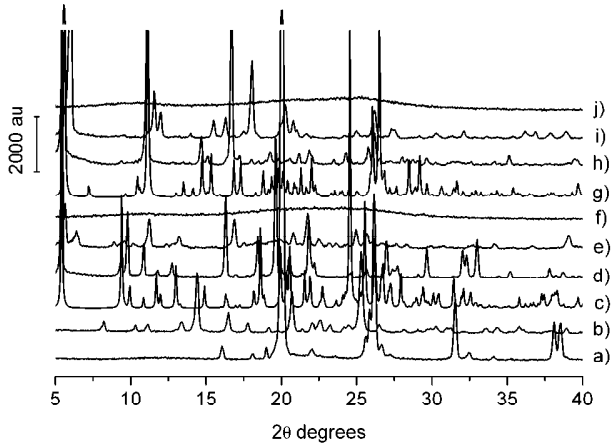

Figure 6. PXRD analysis of: a) C, b) S, c) simulated pattern of CHS-I based on SCXRD, d) CHS-I, e) CHS-II and f) CHS-III, g) simulated pattern of CS-I based on SCXRD, h) CS-I, i) CS-II, j) CS-III.

Anhydrous forms of CHS and CS (CHS-II and CS-II, respectively) had their own, distinct diffraction patterns. CHS-II (Fig. 6e) had the characteristic peaks appearing at 6.41, 11.25, 16.89 and 24.97 2θ degrees, while CS-II (Fig. 6i) presented a PXRD with the characteristic peaks at 6.02, 11.56, 11.98, 15.52, 16.30 2θ degrees.

Thermal properties and water content of the samples are provided in Table 2. The melting point of S was 186.9±0.1 °C (Fig. 7.Ia) while that of C was 265.3±0.6 °C (followed by thermal decomposition, Fig. 7.IIb). The endotherm of dehydration of C-I had an onset at 91.8±0.1 °C and this process was followed by melting with decomposition at 268.4±0.5 °C (Fig. 7.Ic). The first endotherm corresponded to a TGA mass loss of 17.3±0.7% (Fig. 7.IIc), which was consistent with the theoretical water content of 16.6% (Table 1).

Table 2 Thermal properties and water content of S, C-I, CHS-I and CS-I. N/D – not determined.

Sample	Melting point at 10 ºC/min (melting point at 500 ºC/min) (ºC)	Enthalpy of melting (J/g)	Water content by TGA (%)	Water content by KF (%)
S	186.9±0.1	232.2±3.2	N/D	N/D
C-I	268.4±0.5	N/D	17.3±0.7	17.2±0.5
CHS-I	214.8±0.6 (243.7±1.1)	282.5±4.4	12.6±0.8	11.4±0.2
CS-I	228.1±1.3 (236.6±1.5)	181.0±9.4	8.8±0.9	8.1±0.5

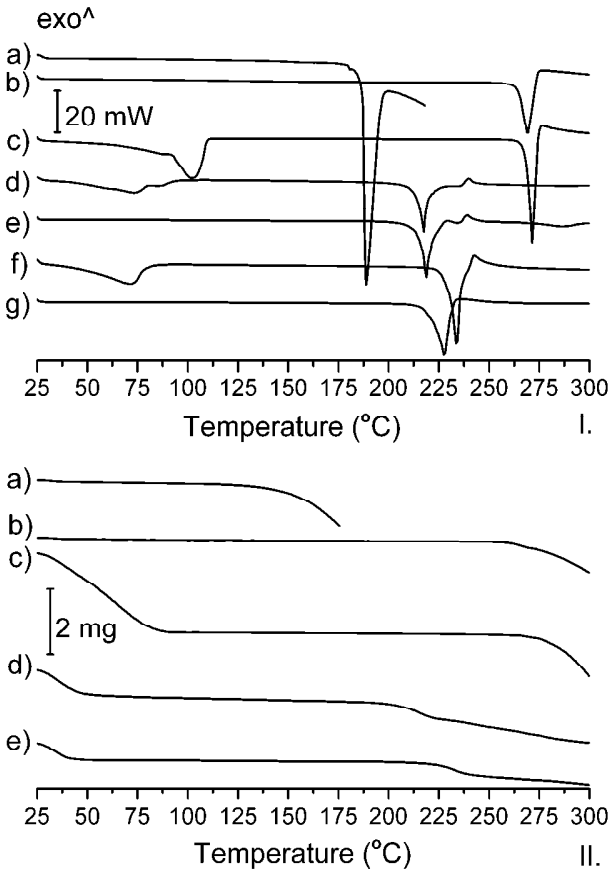

Figure 7. Thermal analysis: I. DSC thermograms of: a) S, b) C, c) C-I (1:3.7 hydrate), d) CHS-I, e) CHS-II, f) CS-I, g) CS-II. II. TGA curves of: a) S, b) C, c) C-I (1:3.7 hydrate), d) CHS-I and e) CS-I.

The DSC scan of CHS-I (Fig. 7.Id) presented an evaporation endotherm with ΔH of 282.5±4.4 J/g corresponding to a TGA mass loss of 12.6±0.8% (equivalent to 3.6 molecules of water per 1 molecule of the salt). The water content by KF titrimetry (Table 2) corresponded to 3.2 molecules of water for 1 molecule of the salt. Therefore the water content in CHS-I agrees well with the crystallography data.

The DSC scan of CS-I (Fig. 7.If) showed a dehydration endotherm with ΔH of 181.0±9.4 J/g corresponding to a TGA mass loss and KF water content (Table 2) equivalent to 4.2 or 3.8 molecules of water per 1 molecule of the salt, respectively. The

number of water molecules determined from the crystal structure analysis is in agreement with the results of thermal and KF analyses within experimental uncertainty. As CS-I was crystallised from 50% v/v ethanolic solution, GC-MS measured that the residual ethanol content was 522±88 ppm. This is in agreement with FTIR findings, as the spectrum of CS-I (Fig. 8.f) does not suggest the presence of ethanol. The melting of CS-I was immediately followed by decomposition (Fig. 7I.f). Thermal analysis showed that the melting point of CS-II form was 220.1±0.9 °C, followed by thermal degradation.

HSDSC was also performed as at a heating rate of 10 ºC/min thermal decomposition of the salts was seen. A gradual shift of the melting point of CHS-I and CS-I to higher temperatures was observed when the heating rates were ramped from 10 to 200 ºC/min. A further increase in the heating rates to 500 ºC/min did not impact on the onset temperature values considerably. Table 2 shows the melting point values for CHS-I and CS-I obtained with the 500 ºC/min rate. HSDSC thermograms for CHS-I and CS-I at different scanning rates are presented in Figures SI.7 and SI.8.

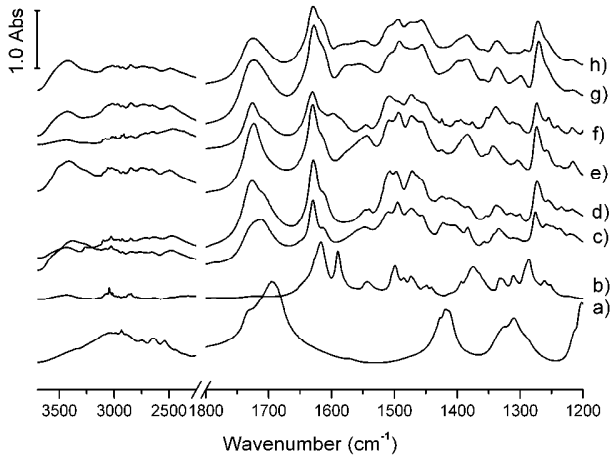

Figure 8. FTIR spectra of: I. a) S, b) C, c) CHS-I, d) CHS-II, e) CHS-III, f) CS-I, g) CS-II and h) CS-III.

The infrared spectrum of C (Fig. 8b) presented characteristic bands at 1617, 1590 and 1375 cm^{-1} assigned to the ketone C=O stretch, antisymmetric and symmetric vibrations of the carboxylate anion, respectively.[50] Hence, the –COOH group of ciprofloxacin was deprotonated in C^{40} in contrast to the crystalline CHS and CS forms (Fig. 8), consistent with SC-XRD data. Protonation of the carboxylic group of ciprofloxacin in the salts was confirmed by the presence of two strong absorption bands at ~1712 cm^{-1} in CHS-I or ~1724 cm^{-1} in CS-I and ~1630 cm^{-1} appearing at similar positions when compared to FTIR of ciprofloxacin·HCl (1709 and 1624 cm^{-1}) and therefore assigned to the carboxylic and ketone C=O group, respectively.[13] The NH group of the piperazine ring was protonated in the crystalline salts and represented by the occurrence of medium intensity bands in the 2400-2700 cm^{-1} region.[13] Very small differences between CHS-I and CS-I were apparent despite the incomplete ionisation of S in the latter, and no band was deemed as sufficiently discriminating (Fig. 8).

Dehydration of CHS-I to CHS-II did not cause major changes in the FTIR spectra, although minor differences were noted in the 1300-1450 cm^{-1} region. In contrast, dehydration of CS-I to CS-II resulted in the appearance of new bands e.g. at 1598 cm^{-1} and 1424 cm^{-1} (Fig. 8g). Also, the band at 1384 cm^{-1} in CS-I was practically invisible in CS-II, instead, a strong band at 1339 cm^{-1} was seen. All these changes indicate modification of the neighbourhood around deprotonated –COOH groups of S, but not C.

3.4 Identification and characterisation of the solid state nature of amorphous salts

The diffractograms of forms CHS-III and CS-III (Figs. 6f and 6j) displayed amorphous halos. The glass transition temperature (Tg) of CHS-III was determined using the PerkinElmer StepScan™ method and was 101.0±0.8 °C (Δc_p 0.46±0.04 J/g). The

amorphous phase was thermally stable up to the onset of crystallisation at 134.2±0.4 °C (ΔH 46.6±0.3 J/g) followed by melting at 202.0±1.9 °C with thermal degradation (Fig. 9).

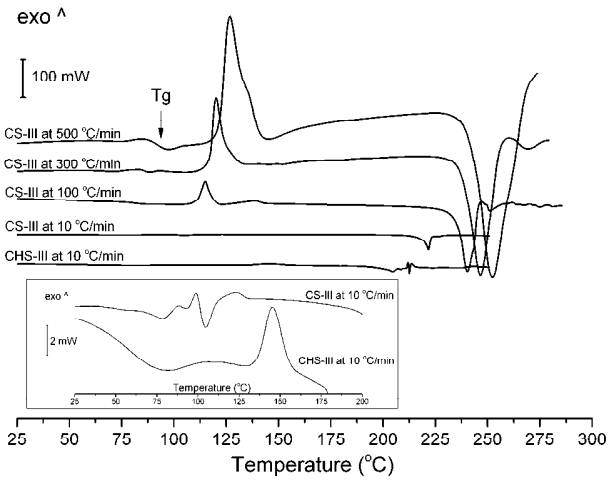

Figure 9. DSC analysis of amorphous salts (CHS-III and CS-III) at different heating rates.

The amorphous phase of CS-III was thermally (physically) unstable. The sample heated at a 10 °C/min rate up to 80 °C in the DSC instrument showed signs of crystallisation to CS-II by PXRD. To avoid a prolonged thermal stress, samples were analysed using HyperScan^{TM} at heating rates of 100, 300 and 500 °C/min (Fig. 9). The use of a heating rate of 100 °C/min was able to prevent cold crystallisation of the amorphous phase. The Tg of CS-III was detected at 81.7±0.6 °C (Δc_p ~0.4 J/g·°C), 86.2±0.8 °C (Δc_p ~0.2 J/g·°C) and 91.7±1.1 °C (Δc_p ~0.5 J/g·°C) at heating rates of 100, 300 and 500 °C/min, respectively. A linear relationship between the heating rates and the T_gs was found (R^2=0.997), and the extrapolated Tg at a 10 °C/min heating rate was determined to be 79.29 °C. The Tg was followed by a crystallisation exotherm to CS-II with an onset at 111.0±0.3 °C, 117.1±0.5 and 121.6±0.2 °C at a 100, 300 and 500 °C/min heating rate, respectively. Melting occurred between ~236 and ~242 °C. Guerrieri et al. calculated that the Tg/Tm ratio for procaine salts varied between 0.68-0.82.[14] The ratios

for CHS-III and CS-III are 0.77 and 0.70, respectively. Ciprofloxacin on its own was, unfortunately, not seen to amorphise completely on milling, neither was it possible to use spray drying (due to the very low solubility of the drug) or quench cooling (due to the thermal decomposition on melting) to produce the disordered form for characterisation.

The FTIR patterns of CHS-III and CS-III were essentially superimposable with small differences in intensity of some peaks in the fingerprint region (e.g. the band at 1299 cm^{-1}) due to the different drug to acid composition (Fig. 8). Similarly to the crystalline salts, the -NH group of the piperazine ring was protonated and represented by the occurrence of medium intensity bands in the 2400-2700 cm^{-1} region. The carboxylic group of the drug was also protonated in CS-III and CHS-III as FTIR showed a strong –C=O band at ~1700 cm^{-1}. FTIR therefore confirmed the ionic nature and proton transfer between the species in the amorphous materials produced either by spray drying or milling with no evidence of different amorphous phases formed by ionised and unionised drug. The existence of a single Tg for CHS-III and CS-III (Fig. 9) also evidenced the mix homogeneity.

3.5. Morphology of the salts

Scanning electron micrographs of CHS-I, CS-I and spray dried systems (amorphous and crystalline) are presented in Fig. 10.

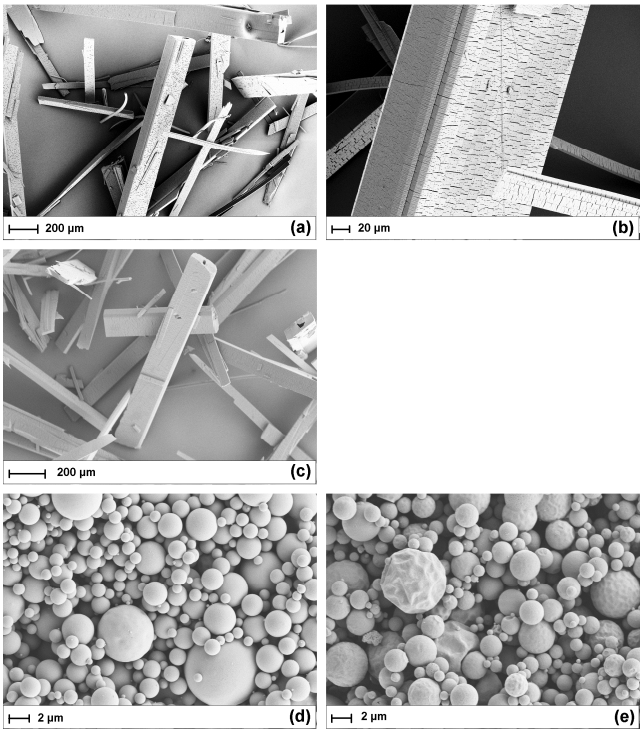

Figure 10. SEM images of: a) and b) CHS-I, c) CS-I, d) CHS-III and e) C and S spray dried in the molar ratio of 1:1 (crystalline).

Calculation of crystallite shapes based on the PXRD pattern derived from SCXRD (theoretical) and measured (experimental) data indicated that the crystals of CHS-I were elongated and formed rectangular prisms (Fig. SI.9). The theoretical crystallite (based on the PXRD derived from SCXRD data) consisted of three principal planes: (201), (001) and (010), corresponding to the respective Bragg peaks at 24.70, 5.45 and 9.45 2theta degrees. A prism of similar shape was determined, based on the experimental data with elongation along the a-axis showing the (022), (001) and (10-2) planes corresponding to the Bragg peaks at 19.60, 5.40 and 16.30 2theta degrees. This morphology is consistent

with that presented in Fig. 10. The crystallite shape calculated for the crystalline spray dried sample (sample g) showed appearance of extra planes: (001), (022) and (201) in addition to main (10-4) and (211) planes (Fig. SI.9) resulting in adoption of less acicular morphology. In this case the growth of each face of the crystal was more uniform, as expected when each particle is formed from a single droplet of solution and indicates that spray drying may be useful as a crystallisation process to overcome the crystal habit issues associated with elongated needles.[51]

The morphology of CS-I based on SCXRD data indicated that prisms were formed and were composed of three major planes: (141), (101) and (001) corresponding to the Bragg peaks at: 26.50, 11.15 and 5.60 2theta degrees (Fig. SI.10). Calculation of the crystal shape from the experimental PXRD pattern indicated that the crystals were more elongated along the b-axis in comparison to those estimated from SCXRD, as seen in SE micrographs presented in Fig. 10.

3.6 Solid state stability of crystalline and amorphous salts

C and C-I were subjected to DVS studies which indicated that, in isothermal conditions of the DVS experiment (25 °C), C did not convert to C-I or any other reported hydrated form of the drug (Fig. SI.6). C, in the range of 0-90% RH, adsorbed only up to 0.6% w/w water (Fig. SI.11). The PXRD patterns of C equilibrated to a constant mass in 0% RH and 90% RH indicated no solid state transformation (Fig. SI.6). In contrast, C-I subjected to DVS studies and equilibrated to a constant mass at 0% RH dehydrated, losing approximately 17% of the initial mass (m_0). This dehydration resulted in a slight change in the PXRD pattern of the material, as observed by the disappearance of the peak at 6.5 2theta degrees (Fig. SI.6). Rehydration of the material was very rapid and was

complete at 20% RH, after which the hydrate remained stable in the range of 20-60% RH. A further increase in the relative humidity up to 90% RH resulted in adsorption of an additional amount of water to 25% w/w of m_0. This second-stage mass increase did not result in a change of the PXRD pattern of the material, which may indicate that water was adsorbed only on the surface of the powder, or that the C-I crystal lattice has a capacity to accommodate additional molecules of interstitial water in the empty voids, as was reported previously for hydrates of chlorothiazide sodium and potassium.[43,52] Such interstitial molecules of water do not change the crystal structure of the hydrate. The hydrated C-I form was stable and did not undergo dehydration up to 10% of RH (Figs. SI.6 and SI.11).

CHS-I subjected to DVS studies dehydrated between 30% and 0% RH losing approximately 11% of water (Fig. 11I). This dehydration was related to a change in the PXRD pattern assigned to crystallisation of CHS-I into CHS-II (Fig. SI.12). The hydration of CHS-II in DVS started slowly, reaching only approximately 5% of m_0 up to 60% of RH and gradually increased to over 10% m_0 at 70% RH forming hydrated CHS-I (Figs. 11I and SI.12), stable in the range from 90% to 30% of RH.

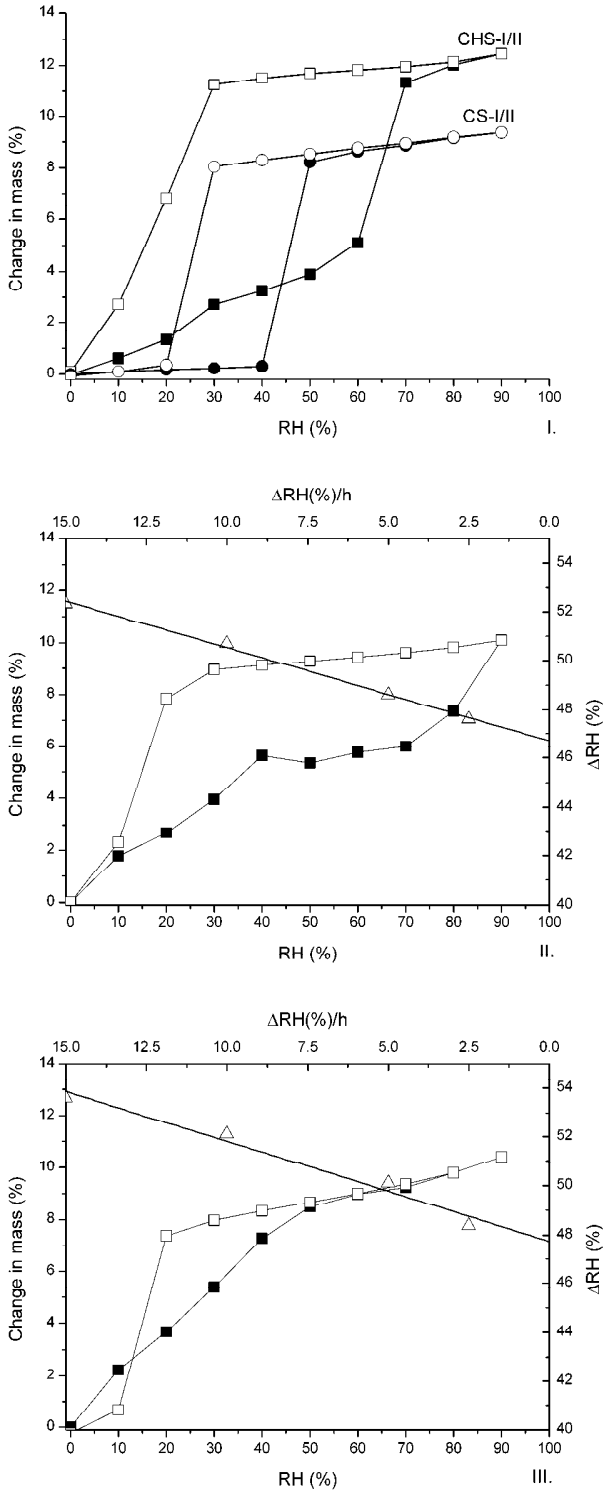

Figure 11. DVS analysis of: I. CHS-I/II (squares) and CS-I/II (circles), II. CHS-III (R^2=0.997, CRH= 46.7%) and III. CS-III (R^2=0.973, CRH= 47.7%). Filled symbols – adsorption, empty symbol – desorption, triangles – critical humidity determination data.

CS-I subjected to DVS studies was demonstrated to be stable in the range of 30-90% RH (Figs. 11I and SI.12). Below 30% RH CS-I dehydrated and crystallised to CS-II form (Fig. SI.12). CS-II was much less hygroscopic in comparison to CHS-II, perhaps due to a greater amount of the hydrophobic drug. It adsorbed less than 1% of m_0 up to 40% RH (Fig. 11I). Between 40 and 50% RH CS-II gradually sorbed approximately 8% of water and crystallised to CS-I (Figs. 11I and SI.12).

DVS studies on the CHS-III form indicated that the amorphous phase subjected to equilibration to a constant mass in the range from 0 to 90% of RH was stable up to 40% RH, sorbing approximately 5-6% m_0 of water and crystallised in the RH range of 40-50% (Figs. 11II and SI.14). The results are consistent with the findings of another DVS experiment where crystallisation of the amorphous material was investigated using fixed rates of RH changes (2.5 to 15% RH per hour)[7] and not the method of equilibration to a constant mass. This experiment confirmed that the critical relative humidity of crystallisation was 46.7±0.9% (Fig. 11II) and the sample transformed to CHS-I.

The mass change magnitude in the DVS studies of CS-III was low and not discriminatory enough to record the mass change related to crystallisation of the amorphous phase (Fig. 11III). The critical relative humidity of crystallisation was determined to be 47.7±0.5% RH in studies which involved subjecting the material to changing RH rates (2.5-15% RH per hour) (Fig. 11III). The amorphous phase was stable up to 40% RH, but at 40% RH it crystallised forming CS-I, which was stable up to 90% RH (Fig. SI.14). In the dehydration cycle the CS-I form was seen to dehydrate to CS-II at 0% RH.

3.7 Solution stability and equilibrium solubility

CHS-I was stable in water and 50% v/v ethanol/50% v/v water with measured total solubilities of 17.4±1.1 and 16.6±2.7 mg/ml, respectively (Table 3). Congruent solubility was observed and the solid phase recovered after the experiment was identified as the starting material. In pure ethanol the components of CHS-I dissolved incongruently and the solid phase was identified as a mix of CHS-I and C. CS-I in water and 50% v/v ethanol/50% v/v water was observed to convert to a mix of C-I and CHS-I instantaneously (Table 3). CS-I was the stable form in terms of the solid state properties when mixed with pure ethanol.

Table 3 Solubility of salts/transformation products in water, ethanol (EtOH) and 50% water/50% ethanol v/v mixture (50% EtOH) at 25 ºC. C-ciprofloxacin, S-succinic acid.

Salt	Solvent	C concentration in liquid phase (mg/ml)	S concentration in liquid phase (mg/ml)	C:S stoichiometry in solution	Solid state phase recovered after experiment
CHS-I	water	12.8±0.9	4.7±0.2	1:1.02	CHS-I
CHS-I	50% EtOH	12.1±2.4	4.6±0.3	1:1.08	CHS-I
CHS-I	EtOH	0.01±0.01	2.8±0.1	1:78.5	CHS-I + C
CS-I	water	14.5±0.2	5.4±0.1	1:0.99	CHS-I + C-I
CS-I	50% EtOH	7.6±0.9	3.2±0.3	1:1.20	CHS-I + C-I
CS-I	EtOH	0.30±0.01	0.14±0.01	1:1.33	CS-I

CS-I was seen to undergo a water-mediated transformation yielding CHS-I and C-I when placed in aqueous solutions (Table 3). It was determined that the CS-I form was stable for at least 24 h in water/ethanol mixes containing at least 80% v/v ethanol. However, as no conversion of CS-I to CHS-I was observed in DVS studies, this water-

mediated transformation may be water activity dependent, similar to the transition of C to C-I.[53]

The ternary phase diagram measured at 25 °C for the ciprofloxacin-succinic acid system in water is presented in Fig. 12. Six regions were distinguished; these represent a single phase of undersaturated solution, so called liquidus (I) and five mixed, solid-liquid phases where the solids exist in equilibrium with solutions: ciprofloxacin (as C-I) (II), a C-I and CHS-I mix (III), CHS-I (IV), a CHS-I and S mix (V) and S (VI). Two eutectic points, E1 (15.2 mg/ml drug and 5.3 mg/ml acid) and E2 (12.7 mg/ml drug and 75.1 mg/ml acid), are also marked on the phase diagram. Since there is an over 2000-fold difference in the aqueous solubilities of the pure components (0.03±0.00 mg/ml for ciprofloxacin (as C-I) and 66.8±4.1 mg/ml for S at 25 ºC), one would expect a highly unsymmetrical ternary phase diagram. However, as the components are able to ionise and impact on each other's solubility, the liquidus region expanded on the ciprofloxacin-rich side of the phase diagram (Fig. 12). The stoichiometric line representing the 1:1 ciprofloxacin: acid molar composition traverses the phase diagram through the region IV only, indicating no drug precipitation during dissolution of CHS-I.

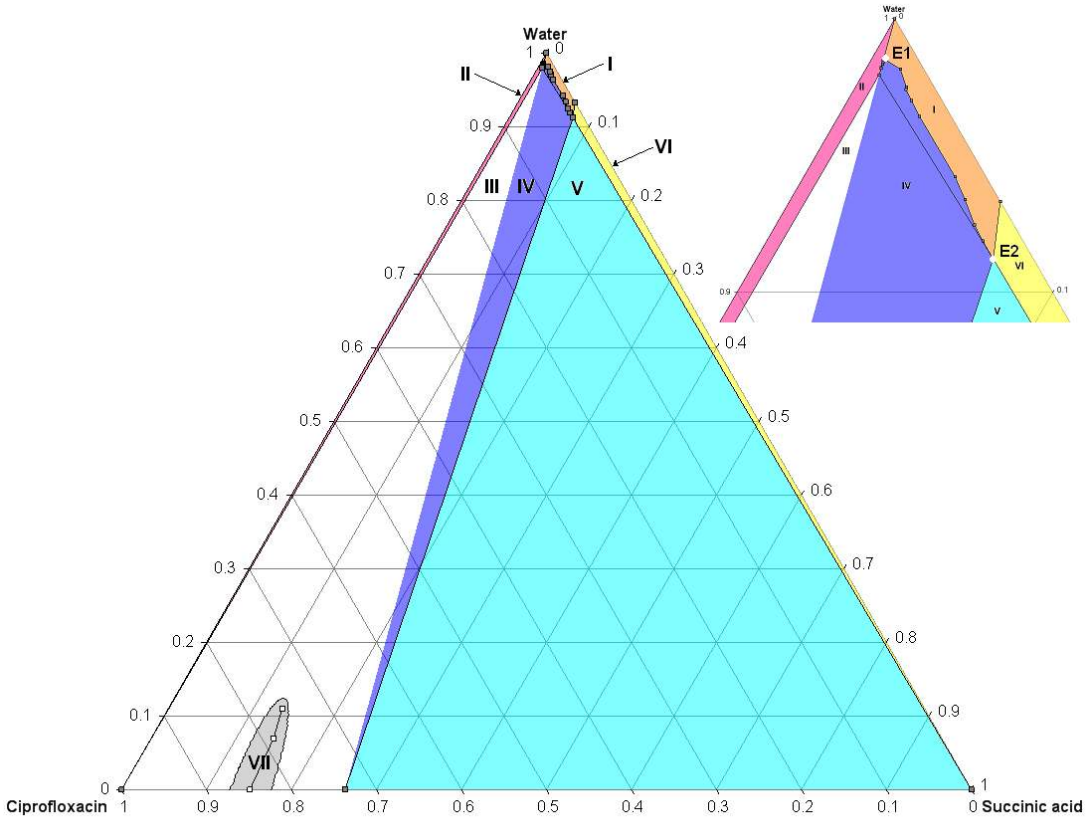

Figure 12. The ternary phase diagram for ciprofloxacin-succinic acid-water system at 25 ºC in mass%. (I) undersaturated solution of ciprofloxacin and succinic acid, (II) ciprofloxacin + liquid, (III) ciprofloxacin + CHS-I + liquid, (IV) CHS-I + liquid, (V) CHS-I + S +liquid, (VI) S + liquid. The shaded area (VII) with empty squares denotes the approximate zone in which the metastable CS-I salt formed from CS-III appears. E1 and E2 are the two eutectic points (white circles). The inset on top right is the enlarged upper part of the phase diagram.

As CS-I was unstable in water and converted to CHS-I and C-I, its position on the phase diagram was marked only tentatively, based on the information collected during DVS analysis of CS-III (as described in Section 3.6 above). It can be estimated whether a salt formed is thermodynamically stable in a solvent by estimating its free energy (ΔG_{salt}, Eqn.1)[54]

$$\Delta G_{salt} = RT \ln\left(\frac{K_{sp}}{10^{pK_C - pK_S} \cdot S_C^m \cdot S_S^n}\right) \quad \text{Eqn. 1}$$

where R is the gas constant, T is the temperature, K_{sp} is the solubility product of the salt, pK_C and pK_S are the dissociation constants of ciprofloxacin and succinic acid in a given solvent, m and n are numbers indicating stoichiometry of the salt while S_C and S_S are molar solubilities of C and S in a given solvent.

For CS-I to be thermodynamically stable, the following condition has to be fulfilled (Eqn.2)[54]:

$$K_{sp} < 10^{pK_C - pK_S} \cdot S_C^m \cdot S_S^n \quad \text{Eqn. 2}$$

In water at 25 °C the K_{sp} for CHS-I was $153*10^{-5}$ M^2, while the pK_C and pK_S difference is 1.88, taking the first ionisation constants of the components, giving $401*10^{-5}$ M^2 for the right hand side part of Eqn.2 (Table 4). Therefore CHS-I is stable in aqueous solutions. The K_{sp} for CS-I was estimated from the dynamic solubility studies and was $44.8*10^{-5}$ M^3, while the $10^{pK_C - pK_S} \cdot S_C^m \cdot S_S^n$ value was equal to $0.038*10^{-5}$ M^3 (Table 4), thus confirming that CS-I is unstable in water. A summary of the values is presented in Table 4.

Table 4 Solubility, K_{sp} and $10^{pK_C - pK_S} \cdot S_C^m \cdot S_S^n$ values for CHS-I and CS-I in water. Sc and Ss – molar solubilities of C and S, respectively, K_{sp} - the solubility product of the salt, pK_C and pK_S are the dissociation constants of C and S, m and n are numbers indicating stoichiometry of the salt.

Salt	S_C (M)	S_S (M)	K_{sp}	$10^{pK_C - pK_S} \cdot S_C^m \cdot S_S^n$	Physical stability in solvent
CHS-I	$9.36*10^{-5}$	0.565	$153*10^{-5}$ M^2	$401*10^{-5}$ M^2	Stable
CS-I	$9.36*10^{-5}$	0.565	$44.8*10^{-5}$ M^3	$0.038*10^{-5}$ M^3	Unstable

3.8 Dynamic and pH-dependent solubility

The drug solubility in water at 25 and 37 ºC was low, reaching 0.06±0.01 and 0.08±0.01 mg/ml, respectively (Figs. 13I and 13II). Dynamic solubility studies of CHS-I in water at 25 °C showed that saturation was achieved after 1 hour (Fig. 13I). CHS-I dissolved congruently, which was indicated from the 1:1 component stoichiometry in solution. CHS-III reached saturation quicker than CHS-I, after 1 minute. The drug: acid solution stoichiometry was 1:0.97 and the solid phase recovered after the study was CHS-I. CS-I in water at 25 °C showed a peak of drug supersaturation (27.5±0.7 mg/ml) at 60 seconds and this ciprofloxacin solution supersaturation lasted for over 10 minutes, after which the drug concentration was comparable to that of CHS-III (Fig. 13I). A rapid change in the drug:acid solution stoichiometry was seen as initially the ratio was 1:0.63, indicating an excess of ciprofloxacin in solution, then at 10 minutes it was 1:0.97, the same as that of CHS-III. The excess solid recovered from the solubility study suspension was a C-I and CHS-I mix.

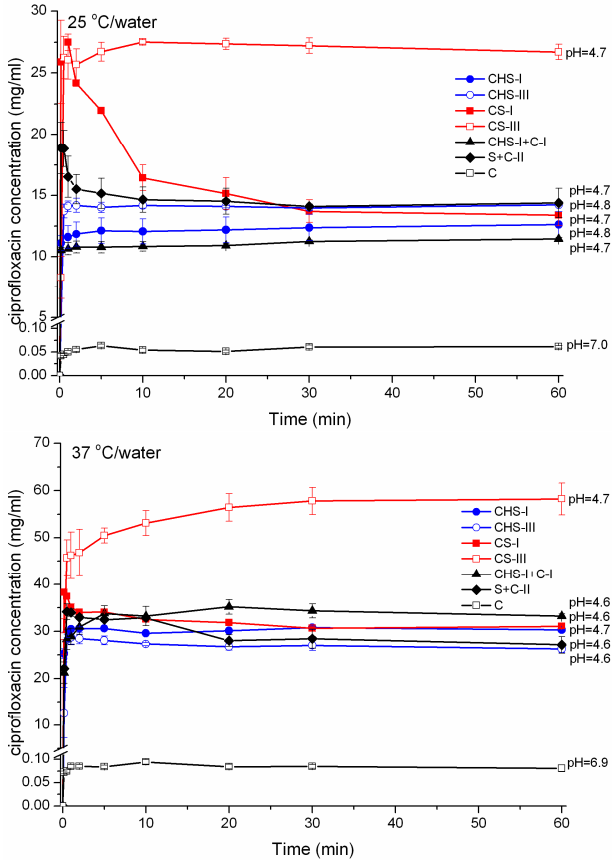

Figure 13. Dynamic solubility studies in water at 25 and 37 ºC. Presented are average values (n=3) and standard deviations as well as solution pH values at 60 minutes of the experiment.

High and sustainable ciprofloxacin levels in solution were attained with CS-III. The solution drug:acid stoichiometry ratios measured over time were anomalous since, at the first time point, after 10 seconds, the drug: acid ratio was 1:0.89, then rapidly decreased to 1:0.56 at 30 seconds and then gradually increased to 1:0.90 at 60 minutes of the experiment. These changes may indicate complex solid-state transformations of CS-III mediated by the presence of water with the possibility of a liquid-liquid phase separation as seen for other poorly soluble drugs[55]. Similarly to CS-I, CS-III in water also converted to a mixture of C-I and CHS-I. A physical mix comprising CHS-I and C-I in a

1:1 molar ratio was also investigated to assess the impact of C-I excess on the salt solubility, however this sample gave the lowest drug concentrations in solution (Fig. 13I). Also, the physical mix composed of S and C in a 1:1 molar ratio was not superior to CS-I and CS-III in terms of drug concentrations measured. The final pH of the saturated solutions formed by the above samples varied between 4.65-4.75 with no obvious trends which would explain the increased drug concentration in solution as a result of pH changes.

The rank order of drug solution concentrations achieved from the various systems at 60 minutes of studies in water at 37 °C was different to that at 25 °C (Fig. 13II). The lowest ciprofloxacin concentrations were obtained from CHS-III and the S/C physical mix, then CHS-I and CS-I followed by the CHS-I/C-I physical mix. Again, the greatest drug concentrations were achieved with CS-III (Fig. 13II). CS-I showed a drug supersaturation (38.3±0.3 mg/ml) at 10 seconds, but lasting only up to 5 minutes, then the drug concentration was comparable to that of the CHS-I/C-I physical mix. A small supersaturation peak was seen for the S/C physical mix. Similarly to the experiments performed in water at 25 °C, the low or high drug solution concentrations could be related to the ratios of molar concentrations of the drug to the acid.

Solubility studies of CHS-I at a pH of 2 and 3.4, where the pH was adjusted using HCl as this ion is present in the gastric fluid, revealed that at the equilibrium (attained after approximately 1 hour) the precipitate/excess salt was made of CHS-I and a hydrochloride salt of ciprofloxacin. The pH-solubility profile of different salts of ciprofloxacin is presented in Fig. SI.17 and suggests that CHS-I may be the better soluble form at higher pH values.

4. Conclusions

In this work we have successfully synthesised crystalline salts of ciprofloxacin succinate, each with a distinct drug/acid stoichiometry and hydration level. The drug was seen to amorphise when co-processed with succinic acid by spray drying or milling yielding amorphous and anhydrous salts with 1:1 or 2:1 stoichiometry, equivalent to the crystalline salts. The proton transfer in both amorphous forms was confirmed by FTIR. The crystalline salts, CHS-I and CS-I, had similar melting points at ~215 and ~228 °C, respectively, while the glass transition temperature of CHS-III and CS-III was ~101 and ~79 °C, respectively.

The ternary phase diagram was demonstrated to be useful in predicting the stability of the crystalline salts in water. Moreover DVS studies complemented these experiments providing information on stability of the various phases at low moisture contents.

The metastable nature of the crystalline ciprofloxacin succinate 2:1 in water led to the attainment of transient drug supersaturation, peaking at 38.3±0.2 mg/ml in water at 37 ºC. The amorphous 2:1 salt was superior to the systems investigated in terms of the solubility behaviour presenting long-lasting drug supersaturation concentrations, characteristic of so-called "spring", but not "spring-parachute" systems.[56] Further studies are required to reveal the biopharmaceutical potential of such supersaturating systems, especially in the context of formulation development.

Supporting information

Supporting Information (SI) material containing additional figures or tables referred to across the manuscript as SI.X are available free of charge via Internet at http://pubs.acs.org.

The Crystallographic information files (CIFs) of CHS-I and CS-I reported in this work (pal02 and pal04 - CCDC 870866 & 870867) are available free of charge from Cambridge Crystallographic Data Centre (CCDC) via: www.ccdc.cam.ac.uk.

Acknowledgements

The authors wish to acknowledge funding for this research from Solid State Pharmaceutical Cluster (SSPC), supported by Science Foundation Ireland under grant number 07/SRC/B1158.

References

(1) Breda, S. A.; Jimenez-Kairuz, A. F.; Manzo, R. H.; Olivera, M. E. Solubility behavior and biopharmaceutical classification of novel high-solubility ciprofloxacin and norfloxacin pharmaceutical derivatives. *Int. J. Pharm.* **2009**, *371*, 106-113.

(2) Harder, S.; Fuhr, U.; Beermann, D.; Staib, A. H. Ciprofloxacin absorption in different regions of the human gastrointestinal tract. Investigations with the hf-capsule. *Br. J. Clin. Pharmacol.* **1990**, *30*, 35-39.

(3) Webb, M. S.; Boman, N. L.; Wiseman, D. J.; Saxon, D.; Sutton, K.; Wong, K. F.; Logan, P.; Hope, M. Antibacterial efficacy against an in vivo Salmonella typhimurium infection model and pharmacokinetics of a liposomal ciprofloxacin formulation. *J. Antimicrob. Agents Chemother.* **1998**, *42*, 45-52.

(4) Turel, I.; Golobic, A. Crystal structure of ciprofloxacin hydrochloride 1.34- hydrate. *Anal. Sci.* **2003**, *19*, 329–330.

(5) Li, S.; Wong, S.; Sethia, S.; Almoazen, H.; Joshi, Y. M.; Serajuddin, A. T. Investigation of solubility and dissolution of a free base and two different salt forms as a function of pH. *Pharm Res.* **2005**, *22*, 628-635.

(6) Reddy, J. S.; Ganesh, S. V.; Nagalapalli, R.; Dandela, R.; Solomon, K. A.; Kumar, K. A.; Goud, N. R.; Nangia, A. Fluoroquinolone salts with carboxylic acids. *J. Pharm. Sci.* **2011**, *100*, 3160-3176.

(7) Paluch, K.J.; Tajber, L.; Elcoate, C. J.; Corrigan, O. I.; Lawrence, S. E.; Healy, A. M. Solid-state characterization of novel active pharmaceutical ingredients: cocrystal of a salbutamol hemiadipate salt with adipic acid (2:1:1) and salbutamol hemisuccinate salt. *J. Pharm. Sci.* **2011**, *100*, 3268-3283.

(8) Storey, R. In *A "roadmap" to solid form selection*; Storey, R. A.; Ymen I., Ed.; Solid State Characterization of Pharmaceuticals, John Wiley & Sons: Chichester, UK, 2011.

(9) Caine D. M.; Paternoster I. L.; Sedehizadeh S.; Shapland, P. D. P. Sequential acetic acid–sodium chloride treatment to control salt stoichiometry of a hydrochloride salt. *Org. Process Res. Dev.*, **2012**, *16*, 518–523.

(10) Kojima, T.; Katoh, F.; Matsuda, Y.; Teraoka, R.; Kitagawa, S. Physicochemical properties of tamoxifen hemicitrate sesquihydrate. *Int. J. Pharm.* **2008**, *352*, 146-151.

(11) Clawson, J. S.; Vogt, F. G.; Brum J.; Sisko J.; Patience D. B.; Dai W.; Sharpe S.; Jones A. D.; Pham T. N.; Johnson M. N.; Copley R. C. P. Formation and characterization of crystals containing a pleuromutilin derivative, succinic acid and water. *Cryst. Growth Des.* **2008**, *8*, 4120–4131.

(12) Stahl P. H.; Wermuth C. G. In *Monographs on acids and bases*; Stahl P. H.; Wermuth C. G., Ed.; Handbook of Pharmaceutical Salts Properties, Selection, and Use, Wiley-VCH:Zurich, Switzerland, 2011.

(13) Parojčić, J.; Stojković, A.; Tajber, L.; Grbić, S.; Paluch, K. J.; Djurić, Z.; Corrigan, O. I. Biopharmaceutical characterization of ciprofloxacin HCl-ferrous sulfate interaction. *J. Pharm. Sci.* **2011**, *100*, 5174-5184.

(14) Guerrieri, P.; Jarring, K.; Taylor, L. S. Impact of counterion on the chemical stability of crystalline salts of procaine. *J. Pharm. Sci.* **2010**, *99*, 3719-3730.

(15) Tong, P.; Taylor, L.S.; Zografi, G. Influence of alkali metal counterions on the glass transition temperature of amorphous indomethacin salts. *Pharm. Res.* **2002**, *19*, 649-654.

(16) Towler, C. S.; Li, T.; Wikstrom H.; Remick D. M.; Sanchez M. V.; Taylor L. S. An investigation into the properties of some amorphous organic salts. *Mol. Pharm.* **2008**, *5*, 946-955.

(17) Sonje, V. M.; Kumar, L.; Puri, V.; Kohli, G.; Kaushal, A. M.; Bansal, A. K. Effect of counterions on the properties of amorphous atorvastatin salts. *Eur. J. Pharm. Sci.* **2011**, *44*, 462-470.

(18) Hasa D.; Voinovich D.; Perissutti B.; Grassi M.; Bonifacio A.; Sergo V.; Cepek C.; Chierotti M. R.; Gobetto R.; Dall'Acqua S.; Invernizzi S. Enhanced oral bioavailability of vinpocetine through mechanochemical salt formation: physico-chemical characterization and in vivo studies. *Pharm. Res.* **2011**, *28*, 1870-1883.

(19) Laudise, R. A. In *The Growth of Single Crystals*; Holonyak, N. Jr., Ed.; Solid State Physical Electronics; Prentice-Hall Inc.: Englewood Cliffs, NJ, 1970.

(20) Büchi 93001 en Operation manual Mini Spray Dryer B-290.

(21) Clark, R. C.; Reid, J. S. The analytical calculation of absorption in multifaceted crystals. *Acta Cryst.* **1995**, A51, 887-897.

(22) Sheldrick, G. M. A Short History of SHELX. *Acta Cryst.* **2008**, *A64*, 112-122.

(23) Blessing, R.H. An empirical correction for absorption anisotropy. *Acta Cryst.* **1995**, *A51*, 33-38.

(24) Tajber, L.; Corrigan, D. O.; Corrigan, O. I.; Healy, A. M. Spray drying of budesonide, formoterol fumarate and their composites. I. Physicochemical characterisation. *Int. J. Pharm.* **2009**, *367*, 79-85.

(25) Momma K.; Izumi F. VESTA 3 for three-dimensional visualization of crystal, volumetric and morphology data. *J. Appl. Crystallogr.* **2011**, *44*, 1272-1276.

(26) Izumi F.; Momma K. Three-dimensional visualization in powder diffraction. *Proc. XX Conf. Appl. Crystallogr., Solid State Phenom.* **2007**, *130*, 15-20.

(27) Tajber, L.; Corrigan, O.I.; Healy, A. M. Physicochemical evaluation of PVP-thiazide diuretic interactions in co-spray-dried composites - analysis of glass transition composition relationships. *Eur. J. Pharm. Sci.* **2005**, *24*, 553-563.

(28) Holubová, J.; Ernošek, Z.; Ernošková, E. The study of the glass transition by the Step Scan DSC technique. *J. Optoelectr. Adv. Mat.* **2005**, *7*, 2671-2676.

(29) Scholz, E. Reagents for Karl Fischer Titration. Springer-Verlag: Berlin, 1984.

(30) Healy, A. M.; McDonald, B. F.; Tajber, L.; Corrigan, O. I. Characterisation of excipient-free nanoporous microparticles (NPMPs) of bendroflumethiazide. *Eur. J. Pharm. Biopharm.* **2008**, *69*, 1182-1186.

(31) Burnett, D. J.; Thielmann, F.; Booth, Determining the critical relative humidity for moisture-induced phase transitions. *J. Int. J. Pharm*. **2004**, *287*, 123–133.

(32) Paluch, K. J.; Tajber L.; Amaro M. I.; Corrigan O. I.; Healy A. M. Impact of process variables on the micromeritic and physicochemical properties of spray-dried microparticles – Part II. Physicochemical characterisation of spray-dried materials. *J. Pharm. Pharmacol.* **2012**, 64, 1583-1591.

(33) British Pharmacopoeia Commission. British Pharmacopoeia. London. **2012**.

(34) Farrugia, L. J. ORTEP-3 for Windows - a version of ORTEP-III with a Graphical User Interface (GUI). *J. Appl. Crystallogr.* **1997**, *30*, 565.

(35) Spek, A. L. Single-crystal structure validation with the program PLATON. *J. Appl. Crystallogr.* **2003**, *36*, 7-13.

(36) Wolff, S. K.; Grimwood D. J.; McKinnon J. J.; Turner M. J.; Jayatilaka D.; Spackman M. A. CrystalExplorer (Version 3.0), University of Western Australia, 2012.

(37) Rodríguez-Hornedo, N.; Nehm, S. J.; Seefeldt, K. F.; Pagan-Torres, Y.; Falkiewicz, C. J. Reaction crystallization of pharmaceutical molecular complexes. *Mol. Pharm.* **2006**, *3*, 362-367.

(38) Trask, A. V.; Haynes, D. A.; Motherwell, W. D.; Jones, W. Screening for crystalline salts via mechanochemistry. *Chem. Commun. (Camb).* **2006**, *7*, 51-53.

(39) Hasa D.; Perissutti B.; Cepek C.; Bhardwaj S.; Carlino E.; Grassi M.; Invernizzi S.; Voinovich D. Drug salt formation via mechanochemistry: the case study of vincamine. *Mol. Pharm.* **2013**, *10*, 211-224.

(40) Fabbiani, F. P. A.; Birger, D.; Florence, A. J.; Gelbrich, T.; Hursthouse, M. B.; Kuhs, W. F.; Shankland, N.; Sowa, H. Crystal structures with a challenge: high-pressure crystallisation of ciprofloxacin sodium salts and their recovery to ambient pressure. *CrystEngComm.* **2009**, *11*, 1396-1406.

(41) Mafra, L.; Santos, S. M.; Siegel, R.; Alves, I.; Almeida Paz, F. A.; Dudenko, D.; Spiess H. W. 2012. Packing interactions in hydrated and anhydrous forms of the antibiotic ciprofloxacin: a solid-state NMR, X-ray diffraction, and computer simulation study. *J. Am. Chem. Soc.* **2012**, *134*, 71–74.

(42) Spackman, M. A.; McKinnon, J. J. Fingerprinting intermolecular interactions in molecular crystals. *CrystEngComm.* **2002**, *4*, 378-392.

(43) Paluch, K. J.; Tajber, L.; McCabe, T.; O'Brien, J. E.; Corrigan, O. I.; Healy, A. M. Preparation and characterisation of novel chlorothiazide potassium solid-state salt forms: intermolecular self-assembly suprastructures. *Eur J. Pharm. Sci.* **2011**, *42*, 220-229.

(44) Somashekar, B. S.; Nagana Gowda, G. A.; Ramesha, A. R.; Khetrapal, C. L. Differential protonation and dynamic structure of doxylamine succinate in solution using 1H and 13C NMR. *Magn. Reson. Chem.* **2004**, *42*, 636-640.

(45) Ravikumar, K.; Swamy, G. Y. S. K.; Krishnan, H. alpha-{3-[2-(Dimethylammonio)ethyl]-1H-indol-5-yl}-N-methylmethanesulfonamide succinate (sumatriptan succinate). *Acta Crystallogr. Sect. E Struct. Rep. Online.* **2004**, *60*, o618-o620.

(46) Maurin, J. K.; Lis, T.; Zawadzka, A; Czarnocki, Z. The crystal structure of strychnidine succinate shows similar self-assembly to strychnine salts. *Acta Crystallogr. Sect. E Struct. Rep. Online.* **2006**, *E62*, o694–o696.

(47) Duggirala, N. K.; Kanniah, S. L.; Muppidi, V. K.; Thaimattam, R.; Devarakonda, S. Polytypism in desvenlafaxine succinate monohydrate. *CrystEngComm.* **2009**, *11*, 989-992.

(48) Kumar, T. L.; Vishweshwar, P.; Babu, J. M.; Vyas, K. Salts of hydrates of imiquimod, an immune response modifier. *Cryst. Growth Des.* **2009**, *9*, 4822-4829.

(49) Bartolucci, G.; Bruni, B.; Coran, S.A.; Di Vaira, M. {2-Hydroxy-3-[4-(2-methoxy-ethyl)-phen-oxy]prop-yl}isopropyl-ammonium hemisuccinate. *Acta Crystallogr. Sect. E Struct. Rep. Online.* **2009**, *65*, o1364-o1365.

(50) Dorofeev, V. L. The betainelike structure and infrared spectra of drugs of the fluoroquinolone group. *Pharm. Chem. J.*, **2004**, *38*, 698-702.

(51) Variankaval, N.; Cote, A. S.; Doherty, M. F. From form to function: Crystallization of active pharmaceutical ingredients. *AIChE J.* **2008**, *54*, 1682–1688.

(52) Paluch, K. J.; Tajber, L.; McCabe, T.; O'Brien, J. E.; Corrigan, O. I.; Healy, A. M. Preparation and solid state characterisation of chlorothiazide sodium intermolecular self-assembly suprastructure. *Eur J. Pharm. Sci.* **2010**, *41*, 603-611.

(53) Li, X.; Zhi, F.; Hu, Y. Investigation of excipient and processing on solid phase transformation and dissolution of ciprofloxacin. *Int. J. Pharm.* **2007**, *328*, 177-182.

(54) Rager, T.; Hilfiker, R. Stability domains of multi-component crystals in ternary phase diagrams. *Z. Phys. Chem*. **2009**, *223*, 793-813.

(55) Ilevbare G. A.; Taylor, L. S. Liquid-liquid phase separation in highly supersaturated aqueous solutions of poorly-water soluble drugs – implications for solubility enhancing formulations. *Cryst. Growth Des.* **2013**, *13*, 1497-1509.

(56) Bak, A., Gore, A.; Yanez, E.; Stanton, M.; Tufekcic, S.; Syed, R.; Akrami, A.; Rose, M.; Surapaneni, S.; Bostick, T., King, A.; Neervannan, S.; Ostovic, D.; Koparkar, A. The co-crystal approach to improve the exposure of a water-insoluble compound: AMG 517 sorbic acid co-crystal characterization and pharmacokinetics. *J. Pharm. Sci.* **2008**, *97*, 3942-3956.

Table of contents/abstract graphic